Wild Gibbon Optimized Sparse Attentive Convolutional Transformer Network for Fault Diagnosis in Electric Vehicles

V. Suresh[1†], **Ch. Leela Kumari**[2], **Marise Satheesh**[3], **Vuyyuru Sri Kavya**[3], and **Nukarapu V V L N Pavani**[3], Non-members

ABSTRACT

Fault Detection and Diagnosis (FDD) is critical for maintaining the security and dependability of Electric Vehicles (EVs). The electric motor drive and battery system, along with the EV's powertrain and energy storage, are essential parts that are susceptible to a variety of malfunctions. Henceforth, this paper presents a fault diagnosis framework dependent on deep learning (DL) and nature-inspired optimization to classify faults with high accuracy. The application uses the NEV Fault Testing Dataset, which contains critical operational signals, including voltage, current, motor speed, temperature, vibration, and humidity signals. Data normalization is applied for ensuring uniformity across the dataset while improving learning capability of model. Exploratory Data Analysis (EDA) is employed for identifying hidden patterns in the dataset and examining the contribution of each variable to the features' distribution. Feature engineering is used for extracting meaningful variables that influence fault-related behavior. The proposed novel model, Wild Gibbon Optimized Sparse Attentive Convolutional Transformer Network (WG-Sparse ACTNet), integrates sparse convolutional methods and attention mechanisms for effective and accurate fault classification while the Wild Gibbon Optimization Algorithm (WGOA) is employed for hyper-parameter tuning to further enhance model accuracy. This model is implemented in Python and evaluated using standard performance metrics, which achieved an accuracy of 99% and a precision, recall, and F1-score of 98%, respectively.

Keywords: Electric Vehicles, Deep Learning, Data Normalization, Exploratory Data Analyses, Wild Gibbon Optimization

---

Manuscript received on October 6, 2025; revised on December 30, 2025; accepted on January 5, 2026. This paper was recommended by Associate Editor Chawasak Rakpenthai.

[1]The author is with Department of Electrical and Electronics Engineering, Godavari Global University, Rajahmundry.

[2]The author is with Department of Electrical and Electronics Engineering, Godavari Global University, Rajahmundry.

[3]The authors are with UG Scholar, Department of Electrical and Electronics Engineering, Godavari Institute of Engineering and Technology.

[†]Corresponding author: sureshvendoti.phd@gmail.com

Digital Object Identifier: 10.37936/ecti-eec.2026241.261696

1. INTRODUCTION

The growing popularity of fossil fuels causes ecological damage and a widespread energy crisis, which has become a global concern. Large-scale advancement of new energy technology is an effective way to address this issue. Among these, EVs are growing into the foundation of the modern energy system [1]. Electrified transportation is a key strategy for reducing carbon emissions, which significantly contribute to climate change and global warming. Furthermore, the scarcity of fossil fuel supplies and the political instability in fossil fuel-producing regions have contributed to global interest in EVs. As the number of EVs is rapidly increasing, and several countries are considering laws to raise EV market share in the coming decade [2-3]. In this context, EV security and dependability are important for achieving a significant market share. It has multiple components, each of which is vulnerable to various forms of failures. Nonetheless, EVs typically arise from primary issues in the battery system and electric motor drive, which are essential parts of EVs [4]. As a result, the effective functioning of these components necessitates careful monitoring, as EV efficiency and security are essential for transportation organizations [5].

However, a variety of issues arise in the motor and drive system because of difficult operating conditions, lowering system functionality, and EV safety and reliability [6]. Electrical motor drive failures occur in three primary categories: mechanical, electrical, and sensor issues, as illustrated in Fig. 1. Electrical issues include open- or short-phase faults, neutralization faults, interturn short faults and open- or short-circuits of inverter's controls [7]. Mechanical errors include rotor-related issues such as bearing issues, broken shafts, and air gap instability. Sensor faults are flaws in various sensors, and early detection is critical for conducting preventative actions to avoid expensive harm and catastrophic failures [8]. EVs often have a variety of electrical and mechanical components that connect via a sophisticated network. Electric motors, control units, and inverter topologies are instances of electrical equipment, while the gearbox and wheel are mostly regarded as mechanical components.

Thus, malfunctions in any part of the mechanical or electrical components, as well as their connections, cause EVs to operate unreliably [9]. As mentioned in [10], EVs experience a variety of fault types, including bearing, rotor, and armature winding issues; inverter or converter issues; and connecting line issues, including single-phase, phase-to-phase, and three-phase issues among the devices, and more. Typically, FDD and classification of EVs are considered using three broad approaches—physical model-based, mapping-based, and data-driven [11]. However, the mapping-based model, which relies on managing data collection from graphs, and the model based, are not suitable for relatively large physical systems, while the data driven model only requires extensive monitored data of the system obtained from varying parameters. In the data driven fault detection and classification methods, data from currents, voltages, speed, temperatures, pressures, and others are gathered to create Machine Learning (ML) based tools for evaluating the condition in various operating instants in the real-time EV driving mode [12].

As a result, academics have performed extensive research in recent decades with the goal of developing safe, dependable, and efficient motor drive systems for EVs. Recently, artificial intelligence involving ML and DL has been employed in improving the EV systems and enhancing the power systems to supply reliable power to customers. A ML-based FDD system has been developed for motors in EV uses a range of different classifiers, such as Support Vector Machine (SVM), k-Nearest Neighbour (KNN), Random Forest (RF), Decision Tree, and XGBoost, to classify both healthy and faulty operating states of motor at fluctuating loads. Nevertheless, the model built within the simulation framework relies extensively on simulated data, which limits its generalizability for real-world fault detection [13-14]. DL models involve Long Short-Term Memory (LSTM) for FDD in EVs to distinguish both short-circuit and open-circuit faults and capture aspects of sensor data, which is an effective solution that avoids concerns with local minima; however, their implementations remain limited to specific failure types and EV components. Also, further evaluation is required to allow for deeper integration with various systems, such as Vehicle-to-Grid (V2G) systems in smart cities [15]. The neural network-based open-circuit fault diagnosis system that employs CNN-LSTM in [16] quickly and accurately generates a high detection rate and reproduces accurately identified faulty conditions, including faults based on phase-to-phase voltage data. However, CNN-LSTM model suffer delay in fault identification when fault signals closely resemble normal signals, thereby compromising real-time acquisition and response for specific incidents.

1.1 Related work

Jiong Yang *et al.* (2022) [17] have introduced a Support Vector Data Description (SVDD) model optimized using Bayesian Optimization (BO) for early recognition of small faults in EV battery systems. This variant of detection performance is superior adjacent to high-dimensional, nonlinear, non-Gaussian data in terms of detecting small, often concealed faults. However, this approach lacks a fault isolation mechanism, making it difficult to precisely identify the sensor from which the fault originated, thereby limiting its effectiveness in fault diagnostics. **Rafia Nishat Toma *et al.* (2020)** [18] have presented a hybrid motor fault diagnostic model based on Genetic Algorithm (GA) combined with an ML classifier. The GA model selects relevant features, significantly reducing dimensionality of the input data, enabling highly accurate classification based on diverse static configurations. Thus, it eliminates the dependency on an external vibration sensor, thereby reducing system cost. However, the approach fails to utilize the diagnostic potential of frequency-domain signal analysis, which is crucial for identifying more complex or less obvious fault signatures in motors. **Wenfang Zheng *et al* (2024)** [19] have implemented a fault analysis based on an Improved Wavelet Packet Decomposition (IWPD) scheme and Chaos-Simulated Annealing Binary Particle Swarm Optimization (CSA–BPSO) to captures fault signal feature and optimize classification. This approach supervised the identification of motor faults with accuracy and recall while requiring a limited loss function and had high fitness values. However, the model is limited to identifying individual fault types without consideration for multiple faults, which reduces its applicability in real systems with complex failure modes. **Ling-Ling Li *et al.* (2021)** [20] have established a fault diagnostic model involving Modified Gray Wolf Optimization (MGWO) combined with Support Vector Machine (SVM) to improve classification outcomes and fault diagnosis in EV motors. The MGWO algorithm enhances and optimizes convergence and robustness in classification. However, the model's reliance on SVM limits its scalability and efficiency when dealing with larger datasets, and its generalizability is still limited due to insufficient testing across a broader range of motor fault scenarios and operating environments. **Venkata Satya Rahul Kosuru *et al* (2023)** [21] have presented an Incipient Bat-optimized Deep Residual Network (IB-DRN) approach for the recognition and classification of false sensor and transmission data in EV Battery Management Systems (BMS). It improves the robustness and safety of the lithium-ion battery system by accurately identifying faulty sensor data. However, the technique has limitations based on the insufficient development of more detailed battery models, failure to visualize sensor data expressed into a learning space, and absence of fault monitoring.

Therefore, in this work, WG-Sparse ACTNet is implemented for a fault diagnosis framework that uses EV sensor data as input to classify various fault types. The contributions of the work are,

- Normalization is used to ensure that all sensor features are on a consistent scale and that the model learns efficiently without being distorted by varying input data magnitudes.
- EDA using distribution plots and correlation is performed for revealing hidden structures, identi-

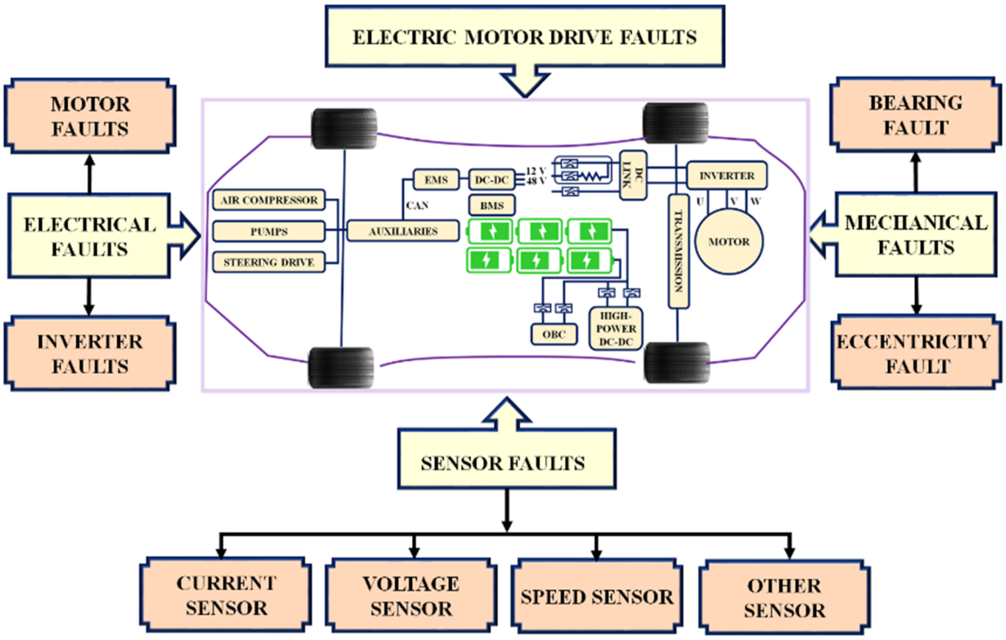

***Fig. 1**: EV motor drive faults.*

fying outliers, and understanding the relationships between relevant sensor measurements.

- Feature engineering to derive useful and discriminating features from the raw sensor signals, which improves the model's capability to differentiate between normal and faulty operating states.
- SAC-TNet as the classifier, which involves sparse convolution and attention paradigms to capture spatial-temporal dependencies for precisely identifying faults.
- WGOA to optimize hyperparameters of the classifier, increasing overall diagnostic accuracy, convergence speed, and model generalization in EV fault classification.

2. PROPOSED METHODOLOGY

The proposed EV fault diagnosis framework exposed in Fig. 2 initiates with the acquisition of sensor data capturing key signals, including voltage, current, temperature, vehicle speed, vibration, and humidity from EV components. These raw sensor data enter the preprocessing stage where normalization techniques are applied to standardize the sensor data, minimize scale-related inconsistencies, and ensure it is suitable for further analysis. Following the pre-processing stage, EDA using distribution plots to visualize trends, outliers, and relationships among variables. This analysis supports the feature engineering stage by identifying meaningful and discriminative features associated with fault behavior. After specific features are engineered, this data input is fed into a SAC-TNet, which acts as a classifier trained to learn spatial-temporal patterns from multivariate sensor data to accurately identify faults in the EV.

To enhance model performance, integrating the WGOA, is employed to fine-tune the classifier's hyperparameters, thereby maximizing classification accuracy. This optimized framework enables real-world detection and classification of motor, inverter, and battery faults in EVs.

2.1 Data Collection

The dataset utilized in this study is from the NEV Fault Testing Dataset, which includes labelled sensor readings from EV parts and components with sensor readings in both normal and faulted states. Important parameters, including voltage, current, motor speed, temperature, vibration, and humidity, are collected. These signals demonstrate both the internal between-component behavior and external operating behavior for the vehicle and are useful to identify faults denoting motor, inverter, and battery faults at a high level. There are significant complexities and overlap in most of the sensor readings due to the nature of each fault type, making it difficult to accurately isolate the fault. This dataset makes it possible to implement a fault diagnosis model that uses multi-sensor reading analysis and classification on the remote EV platform. The proposed framework seeks to investigate whether integrating multiple streams of sensor data using a variety of advanced techniques that characterize sub-categories of faults.

2.2 Preprocessing

2.2.1 Normalization

The fluctuation of input data has a negative impact on the precision of the model's outcome classification. However, the initial information during the scaling process improves the quality of the experimental categorization and the model's precision for classification, thus input

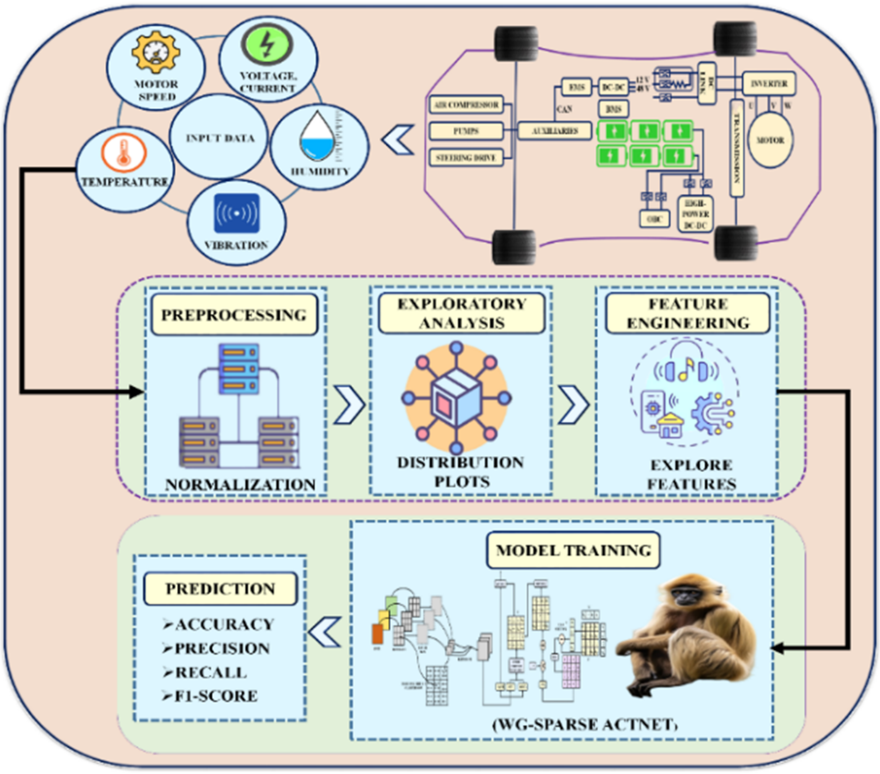

Fig. 2: *Proposed Block of EV fault diagnosis.*

data normalization is essential. The map *min max* function is utilized to handle data, especially training and test data, based on the characteristics of the EV fault current signal. The premise of processing data is stated below.

$$I_{scale,i} = \frac{I_i - I_{min}}{I_{max} - I_{min}} \tag{1}$$

Here $I_{scale,i}$ represents normalized current signal of EV; I represent current signal of EV; and I_{max} *and* I_{min} indicate maximum and minimum values of EV current signal. Data collected from sensors received preliminary processing while being suitable for fundamental processing and examination. Z-score normalization obtaining mean and standard deviation for individual feature in a training set and dividing between numerous variables in training dataset. Each attribute has its own mean and standard deviation. The general formula specifies the transformation to be executed,

$$c = \frac{(c - \mu)}{\sigma} \tag{2}$$

Here, c and μ stand for normalized and mean values and their standard deviation denoted by σ. Once training data has been calculated, it is very important to keep standard deviation and mean of every feature to use as weights in the design of system.

2.3 Explotary Analysis

EDA using distribution plots is important for understanding behavior, spread, and patterns in sensor data. These plots aid in identifying skewness, center of tendency, and outliers exhibited in variables like temperature, voltage, and current, each of which serves as an important predictor of abnormal operating conditions. In addition, outliers indicate early signs of faults, therefore utilizing distribution plots enables early identification of any potential anomalies in temperature, voltage, and current data to ensure reliable diagnosis. Additionally, understanding feature distribution supports identifying which DL models are suitable for analysis, as several models require a normal distribution of the adopting features.

2.4 Feature Engineering

It's a critical step in EV fault diagnosis as it transforms raw multivariate sensor data into salient features that highlight faulty patterns. The multi-parameters are sometimes captured by noisy sensors, including voltage, current, temperature, motor speed, vibration, and humidity. Focusing directly on the raw data make it difficult to detect faults, because the raw recorded data may be noisy or redundant. The primary goal in feature engineering is to extract significant statistical descriptors—such as mean, standard deviation, skewness, and peak/max values—to describe the inherent behavior of each signal. These descriptors assist in detecting deviations from expected operational parameters and help define a fault. Also, the relationships of these variables were analyzed to help identify complex fault signatures. It shows improvement on the data's interpretability, assists in reducing dimensionality, and increases the quality of model input. The process assurances the diagnostic system withstand different environmental conditions and operational situations, while enhance accuracy, and speed faults recognition. The refined features are passed into the classification stage in the pursuit of finding faults.

2.5 Wild Gibbon Optimized Sparse Attentive Convolutional Transformer Network (WG-SPARSE ACTNET)

2.5.1 Sparse Attentive Convolutional Transformer Network (SAC-TNet)

A SAC-TNet is an advanced DL that enables effective fault diagnosis in EVs. SAC-TNet addresses the challenges of efficient multivariate time-series and modeling from complex multivariate time-series sensor data for EVs. It integrates Sparse Convolutional Neural Networks (SCNNs) for capturing local temporal-spatial patterns with transformer networks using a sparse attention mechanism for modeling long-range dependencies and capturing contextual relationships with lower computational costs.

2.6 SCNN

In an SCNN model, conduct a sparse convolutional layer using multiple convolution kernels followed by sparse matrix multiplication. This sparse structure is the basis for implementing the convolutional operations at a greater level of efficiency, provided that the classifier with the capability of performing fast and memory-efficient feature extraction with ideal applicability for real-time fault detection in EV systems. Input feature map and convolutional kernel be denoted as:

$$I \in \mathbb{R}^{h \times w \times m} \tag{3}$$

$$K \in R^{(s \times s \times m \times n)} \tag{4}$$

where h, w and m denotes height, width and number of channels respectively. s denotes the size of the convolutional kernel, and n stands for the number of output channels. The standard convolution operation is expressed as:

$$O(y, x, j) = \sum_{i=1}^{m} \sum_{u,v=1}^{s} K(u, v, i, j) I(y + u - 1, x + v - 1, i) \tag{5}$$

To approximate the convolution and decrease computational complexity, use a sparse version of convolution. To optimize, SCNN decomposes K expressed as,

$$K(u, v, i, j) \approx \sum_{k=1}^{m} R\left(u, v, k, j\right) P\left(k, i\right) \tag{6}$$

Similarly, the input feature map is transformed as:

$$J\left(y, x, i\right) = \sum_{k=1}^{m} P\left(i, k\right) I\left(y, x, k\right) \tag{7}$$

Finally, the output of the sparse convolutional operation becomes:

$$O\left(y, x, i\right) \approx \sum_{i=1}^{m} \sum_{k=1}^{q_i} S_i\left(k, j\right) T_i\left(y, x, k\right) \tag{8}$$

This formulation allows the convolutional layer to be implemented as a series of efficient matrix multiplications. By utilizing sparse, low-rank representations of the convolutional kernels enable the classifier significantly reduces memory usage and implication time, creating it suitable for real-time EV health monitoring systems.

2.7 Sparse Attention Mechanism

Sparse Attention Mechanism is a less computationally expensive implementation by restricting computations to a subset of relevant positions, significantly reducing memory usage and inference time. The resource-constrained applications like EV fault diagnosis, where it preserves essential contextual dependencies while minimizing computational overhead.

This module improves attention efficiency by maintaining only the top k significant attention scores while removing noise from irrelevant features. Given input represents $Q, K, V \in \mathbb{R}^{n \times d}$, the standard attention, which is calculated as:

$$Attention\left(Q, K, V\right) = softmax\left(\frac{QK^T}{\sqrt{d}}\right)V \tag{9}$$

A mask matrix $M \in \{0, 1\}^{n \times n}$ is introduced by sparse attention,

$$Attention\left(Q, K, V\right) = softmax\left(\frac{QK^T \odot M}{\sqrt{d}}\right)V \tag{10}$$

Multiplication by elements is represented by $\odot$. Typically, M is generated using learned sparsity patterns, block/locality-based masks, thresholding, or top-k selection.

2.8 Spatial-Temporal Block Design for Sparse Attentive Classification

The SAC-TNet classifier incorporates Spatial-Temporal (ST) blocks designed to effectively capture both spatial and temporal dependencies from multivariate sensor data in EVs. Each ST block contains a sparse spatial transformer and a sparse temporal transformer, enabling the model to dynamically learn spatial patterns associated with fault conditions and sequential patterns influenced by changes in past EV sensor conditions. The ST blocks are hierarchically stacked to form a deep architecture for learning high-level ST features crucial for accurately classifying faults in EVs.

The output of $(l-1)-th$ block is transmitted into $l-th$ spatial-temporal block at time step$T_{obs} - k + 1$. Block originates with a sparse spatial transformer, which learns

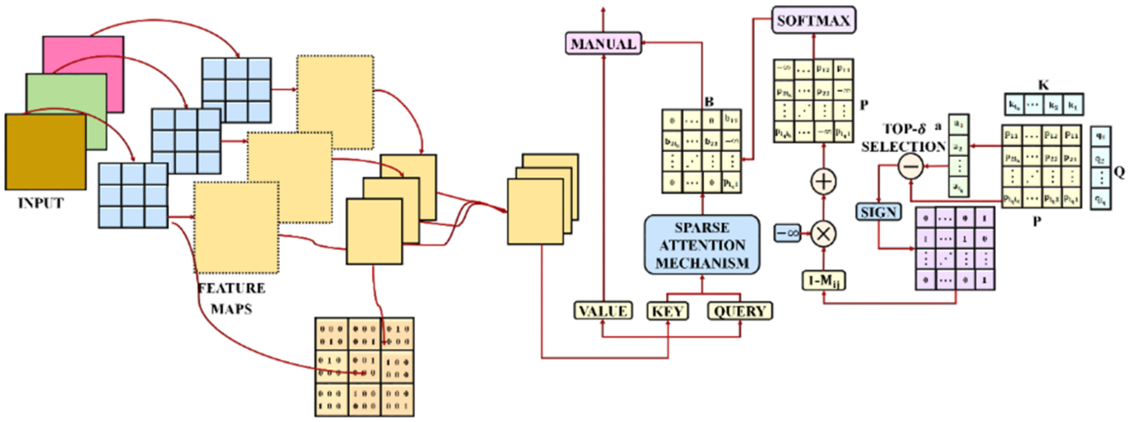

***Fig. 3**: Architecture diagram of SAC-TNet.*

spatial dependencies between multiple sensor channels (e.g., voltage, current, temperature):

$$Y_l^s = S\left(X_l^s\right) \tag{11}$$

Here stands the spatial input tensor and Y_l^s stands output X_l^safter a sparse spatial transformation. This output is then fused with the original input using a residual connection to preserve low-level feature information:

$$X_l^T = Y_l^s + X_l^s \tag{12}$$

The sparse temporal transformer processes the coupled tensor X_l^T, capturing sequential dependencies and fault dynamics over time.

$$Y_l^T = T\left(X_l^T\right) \tag{13}$$

The result Y_l^T is used as input for the following ST blockX_{l+1}^s. This allows the model to refine ST patterns layer by layer. By stacking various ST blocks and combining their outputs in the final prediction layer (a fully connected classifier), the model achieves accurate and accessible fault detection across complicated, multimodal EV sensor streams. These sparse characteristics are subsequently supplied into the SAC-TNet's transformer layers that utilize sparse attention methods to simulate long-range dependencies, resulting in accurate fault classification as illustrated in Fig. 3. This setting enables SAC-TNet classifier to dynamically concentrate on fault-relevant patterns in time-series sensor data, while ignoring irrelevant historical fluctuations. To improve the performance of EV fault diagnosis, WGOA is employed to efficiently tune the classifier parameter.

2.8.1 Wild Gibbon Optimized Algorithm

The WGOA is a bio-inspired metaheuristic that mimics the territoriality and competitive behaviors of gibbon families in the wild. Within the setting of EV fault diagnosis, WGOA is used to optimally tune the hyperparameters and architecture of the proposed SAC TNet to aid in model's capability to more precisely distinguish, generalize, and categorize complex multivariate fault patterns from EV sensor data at lower computing costs. In WGOA, each particle represents a gibbon family, consisting of three memory layers as behavioral representations of members of the gibbon's family:

1. Male memory layer (the local leader): engages in local exploitation as a mechanism to improve good configurations.
2. Female memory layer (the stabilizer): protects near-optimal solutions for stability.
3. Child memory layer (the explorer): provides more salient exploration to remain out of local minima.

2.9 Community Search Strategy

Each particle simulates a gibbon family with three memory layers: male (best), female (second-best), and child (third-best). The male memory leads the search, exploring better positions. If a superior position is found, the group's memories are updated; otherwise, they remain unchanged. Female and child memories ensure a balance between local exploitation and global exploration, enhancing optimization diversity and stability. The community search process directs each gibbon family (particle) to gather and refine model configurations by collaboratively updating its memory layers. Through this searching approach, SAC-TNet is able to efficaciously search the hyperparameter and retain heterogeneous types of configurations that obtain a good balance of accuracy and generalization. The memory layers are updated accordingly to retain the top three configurations per family,

$$\alpha = \frac{Gib_{ii}^t(k) + BestGib^t(l)}{2} \tag{14}$$

$$\beta = \left|Gib_{ii}^t(k) + BestGib^t(l)\right| \tag{15}$$

$$GibCandidate_{ii}^{t+1}(k,l) = GD(\alpha,\beta) \tag{16}$$

$$Gib_{ii}^{t+1} = Best\left(3, \left(GibCandidate_{ii}^{t+1},\ Gib_{ii}^t\right)\right) \tag{17}$$

Every SAC-TNet configuration candidate is characterized by a triple defined by the memory roles $k = 1$

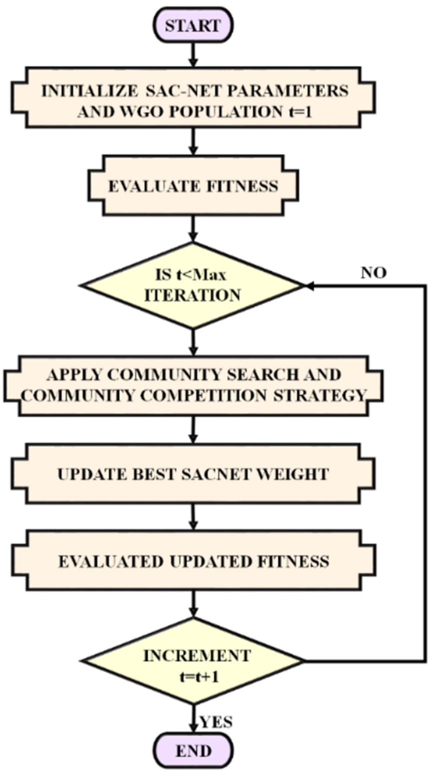

Fig. 4: *Flowchart of WG-Sparse-ACTNET.*

(male), $k = 2$ (female), and $k = 3$ (child). The current position of $k-th$ layer of $i-th$ particle at iteration t can be denoted by $Gib_{ii}^{t}(k)$ and the globally best memory as $BestGib^{t}(l)$. New candidate locations are created using a Gaussian distribution (GD), which has a mean and variance calculated based on the current particle and global best. The updated memory layers are selected using $Best(3,\cdot)$,a function that ranks the configurations and keeps the three best performers. The model uses the three combined search perspectives of male (local leader), female (stabilizer), and child (explorer) to preserve exploration–exploitation balance and to improve convergence. The WG-Sparse ACTNet flowchart, demonstrated in Fig. 4, outlines the step-by-step procedure for fault classification using the optimized DL model.

2.10 Community Competition Strategy

To optimize global performance, the community competition approach ensures that only the best-performing SAC-TNet configurations survive across generations. This process mimics inter-family competition, where only the most efficacious solutions survive and replicate. To increase convergence and local search capability, the approach keeps track of three historical best positions aligned with the memory layers used in the Community Search Strategy. After each generation, the leading particle (i.e., global best memory) explores to search for a new candidate solution for the following generation. If this candidate outperforms the current global best, it replaces it:

$$BestGibCandi^{t+1} = Best\left(Gib_{1}^{t}(1), Gib_{2}^{t}(1), .., Gib_{n}^{t}(1)\right) \tag{18}$$

$$BestGib^{t+1} = Best\left(BestGibCandi^{t+1}, BestGib^{t}\right) \tag{19}$$

In this approach, Gib_{1}^{t} defines the male of $i-th$ gibbon at iteration t. Then evaluate the best positions to select the best one according to its fitness value by means of the $Best(\cdot)$function. Thus, providing continuous improvement to the global best solution of competitive selection.

2.11 Problem formulation of WGOA based hyper-parameter optimization:

To clearly characterize the optimization process, the tuning of the SAC-TNet model is expressed as a constrained optimization problem. The objective of WGOA is to find the best collection of hyperparameters that improve the fault prediction accuracy of the proposed WG-Sparse ACTNet model.

2.11.1 Decision Variables

Define the hyperparameter vector as:

$$X = [\eta, L,\ H,\ B,\ D] \tag{20}$$

Here, η stands for learning rate. L *and* H stands number of network layers and attention heads, B *and* D stands batch size and dropout rate.

Objective Function:

$$\max F(X) = Accuracy(X) \tag{21}$$

Where $F(X)$ denotes the fitness value derived from the SAC-TNet model's ability to classify on the validation dataset using hyperparameter set X. The objective is frequently expressed as a minimization of error:

$$\min E(X) = 1 - Accuracy(X) \tag{22}$$

2.11.2 Constraints

The following constraints apply to the optimization:

$$\eta_{min} \le \eta \le \eta_{max} \tag{23}$$

$$L_{min} \le L \le L_{max} \tag{24}$$

$$H_{min} \le H \le H_{max} \tag{25}$$

$$B_{min} \le B \le B_{max} \tag{26}$$

$$0 < D < 1 \tag{27}$$

2.11.3 Fitness Evaluation

The SAC-TNet model is trained with the matching hyperparameter configuration X for each potential solution produced by WGOA. The fitness value is derived from the classification accuracy on the validation dataset. To optimize the fitness function, the WGOA algorithm iteratively updates the candidate solutions using community search and competition strategies. This formulation

***Table 1**: Pseudo code for WGOA.*

WGOA
Require:
    Fitness function F ,
    Maximum number of evolutions T ,
    Gibbons $Gib = \{Gib(1), Gib(2), ..., Gib(n)$,
    Leader of gibbons, BestGib
    Personal best positions, P_{best} history
    Global best position, G_{best} history
Initialize:
    Set memory layers $mm = 3$
    Each Gib contains mm memory layers
Memory Initialization:
    For mm=1 to 3:
    Calculate positions using fitness F
    Record results as
    $Gib(1)(mm), Gib(2)(mm), \ldots, Gib(n)(mm)$
    End For
    Sort memories of each gibbon
    Place best positions in the first layer
    Place worst positions in the last layer
Optimization Loop:
Set $t = 1$
While $t < T$:
    Apply Community Search Strategy
    Apply Community Competition Strategy
    $t = t + 1$
End While
Output:
    Choose the best gibbon from Gib
    Return BestGib

implies that WGOA directs the search process into globally optimal fault diagnostic performance and expressly optimizes the crucial training parameters of SAC-TNet.

Table 1 illustrates pseudocode for WGOA, which describes the essential processes in initializing, updating, and selecting optimal solutions throughout the optimization process. This approach ensures that only the best solutions from the population are retained, which helps the SAC-TNet classifier perform better in diagnosing EV faults. In regard to model configuration, this supports global optimality and effective convergence. Table 2 lists the hyperparameter settings utilized in the proposed WG-Sparse ACTNet model for training and optimization.

3. RESULT AND DISCUSSION

The proposed WG-Sparse ACTNet model was developed with Python and tested on the NEV Fault Testing Dataset, which was split into 70% training and 30% testing. The model performed an excellent task of classifying faults in motors, inverters, and batteries, with high accuracy, precision, recall, and F1-score.

***Table 2**: WGOA hyperparameters specifications.*

Hyperparameters	Value used
Number of whales	30
Iterations	50
Learning rate	0.001
Number of Layers	4
No. of Attention Heads	4
Batch Size	32
Dropout Rate	0.3
Activation Function	ReLU

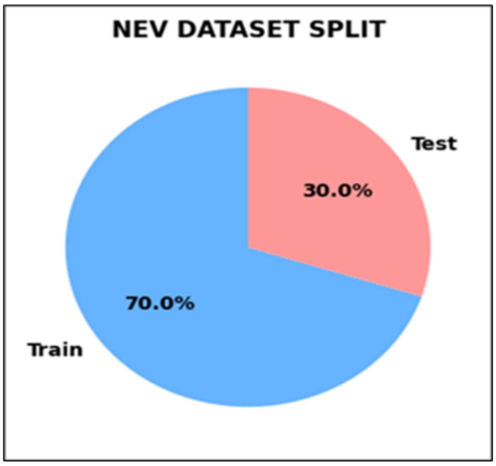

***Fig. 5**: NEV Dataset Split.*

Dataset Details

Dataset Shape: 11000 ROWS AND 8 COLUMNS
Dataset Columns: Voltage (V), Current (A), Motor Speed (RPM), Temperature (°C), Vibration (g), Ambient Temp (°C), Humidity (%), Fault Label
Input (X): Voltage (V), Current (A), Motor Speed (RPM), Temperature (°C), Vibration (g), Ambient Temp (°C), Humidity (%)
Output (Y): Fault Label
Test-Train Split: 70% TRAIN -30% TEST
Train Counts: 7700
Test Counts: 3300

Fig. 5 indicates data partitioning of the NEV Fault Testing Dataset, with 70% of data (7700 samples) used to train the proposed model and 30% of data (3300 samples) reserved for testing to assess the fault diagnosis framework's generalization performance.

Fig. 6 illustrates the distribution of the fault labels in the NEV dataset. The dataset contains a total of four classes: 0, NORMAL; 1, MOTOR FAULT; 2, INVERTER FAULT; and 3, BATTERY FAULT. The relatively comparable distribution of the three fault classes (each 18.2%) and the normal class (45.5%) minimizes class imbalance throughout training and prevents model bias toward dominant classes. This balanced structure allows the classifier to learn meaningful decision boundaries for each fault category, enhancing convergence dependability,

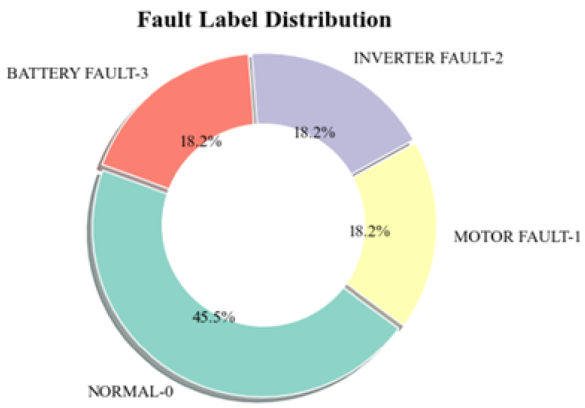

***Fig. 6**: Fault Label Distribution.*

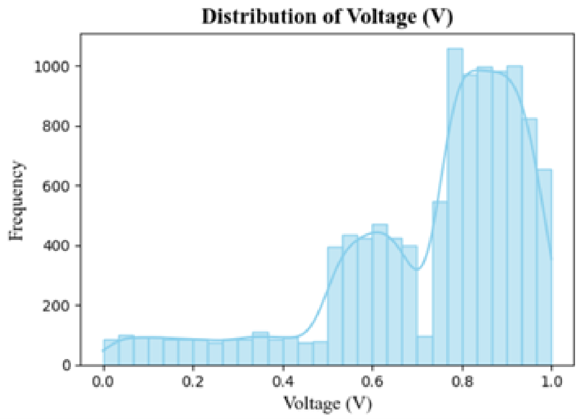

***Fig. 7**: Distribution of Voltage.*

classification reliability, and generalization performance across previous EV operating circumstances.

Fig. 7 supplies essential technical information on the voltage behaviour of the EV system under numerous operating and fault conditions. The observed multi-modal voltage distribution demonstrates the presence of several operational states, including both healthy and fault scenarios. This variation in voltage patterns presents substantial discriminative information to the proposed model, allowing the sparse convolution and attention processes of WG-Sparse ACTNet to efficiently learn fault-relevant voltage signatures and increase classification accuracy.

Fig. 8 presents the distribution of current values (A) across the dataset. The histogram is left-skewed, with the current values from 0.2 to 0.4 having the most frequency. This shows that the current readings are in the lower to mid-ranges for most current values, which is consistent with regular or low-load driving conditions. These differences in current patterns provide crucial information for the proposed model to differentiate between healthy and fault states, increasing the sensitivity and robustness of the fault diagnostic procedure.

Fig. 9 density plot shows the humidity levels from humidity data (%) in the NEV dataset. The density plot shows nearly complete distribution across the entire

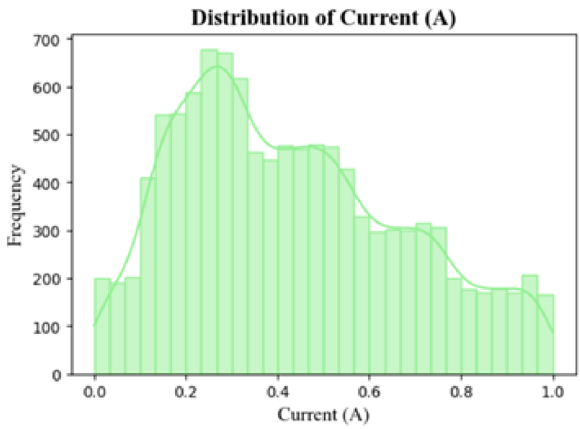

***Fig. 8**: Distribution of current.*

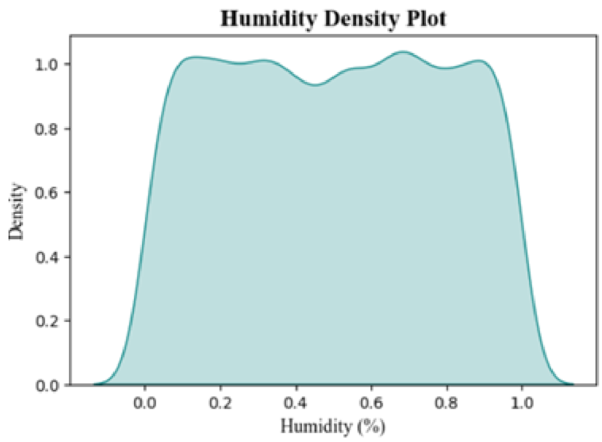

***Fig. 9**: Humidity Density plot.*

range up to 1, and demonstrates well-balanced humidity values across a range of environmental conditions. This diversity reduces environmental bias, increases the capacity for generalization of the WG-Sparse ACTNet model, and increases its durability when deployed in real-life scenarios where humidity variations have a substantial impact on sensor behavior and fault characteristics.

Fig. 10 presents a statistical summary of vibration signals (g) within the NEV dataset that has the minimum, maximum, mean, and standard deviation of the vibration feature listed. The data suggest a minimum value of zero, a maximum value of 1.000, a mean value of 0.281, and a standard deviation of 0.241, which suggests a moderate amount of variability in vibration signals across a driving or fault scenario.

Fig. 11 demonstrates the correlation heatmap between various sensor parameters and the fault label. The correlation magnitude is represented with a color scale indicating the direction from -1 (strong negative) to +1 (strong positive). The voltages (V) have the strongest negative correlation (-0.84), while temperature ($^{\circ}C$) has a positive correlation (**??**), while the other variables (currents, speed, and vibration) have weaker or negligible correlations. This insight helps prioritize features during

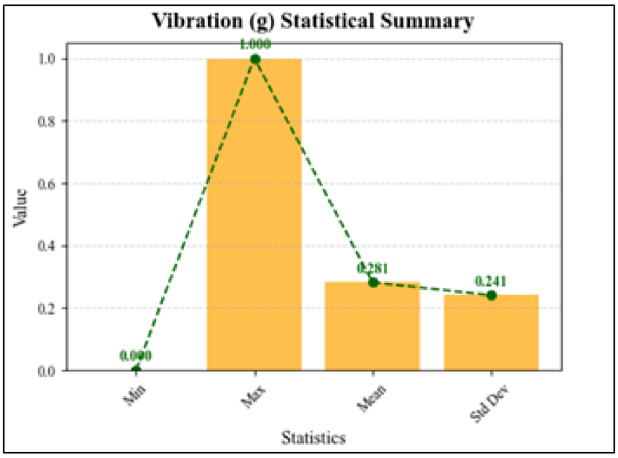

***Fig. 10**: Vibration Statistical summery.*

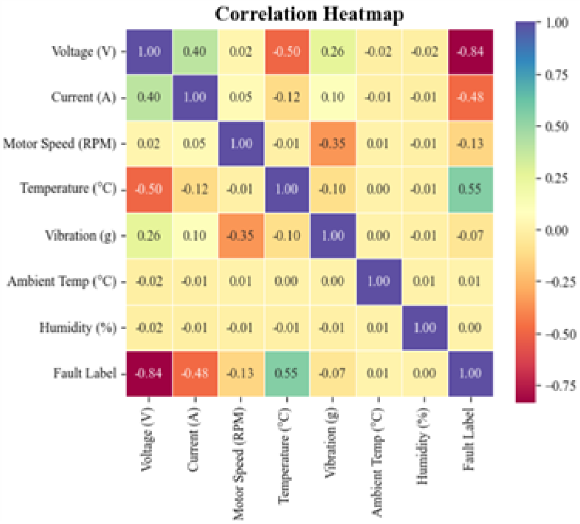

***Fig. 11**: Correlation Heatmap.*

model training and interpretation.

Fig. 12 demonstrates the training performance of the proposed WG-Sparse-ACTNet model trained over 50 epochs. In the model loss curves for training and validation datasets, they converge rapidly, reaching near zero, indicating that the model learned quickly with minimal overfitting. In the accuracy curves, they are shown, and the training and validation accuracies exceed 99% and remain stable, indicating an excellent generalization performance.

Fig. 13 represents a computational time analysis of the proposed WG-Sparse ACTNet model, displaying the average training time per epoch. The computational efficiency of the suggested WG-Sparse ACTNet model is tested to determine its suitability for real-time EV fault diagnostics. The average training time per epoch exceeded 12 seconds, and the average testing time per sample is 2.1 milliseconds, demonstrating that the proposed model is capable of rapid and reliable fault classification in real-time EV applications.

Fig. 14 displays a confusion matrix from the WG-Sparse-ACTNet model on the NEV test data and indicates a greater level of classification accuracy, particularly for the NORMAL-0 class with 1510 correct predictions and reliability with fault classes. Minor misclassifications are observed between classes 2 and 3, indicating slight confusion between INVERTER FAULT-2 and BATTERY FAULT-3. Overall, this model concluded that the greater ability to discriminate between fault categories.

The Receiver Operating Characteristic (ROC) curve for the multiclass classification is shown in Fig. 15. ROC curve shows the balance of trade-off between true positive rate, and false positive rate for each class. AUC (area under the curve) shows almost perfect model classification results with AUC values of 1.000000 for (NORMAL-0) and (MOTOR FAULT-1), 0.999229 for (INVERTER FAULT-2), and a value of 0.999220 for (BATTERY FAULT-3). These findings support the model's unique classification performance, with minimal false positives across all the fault categories.

Fig. 16 represents an analysis of classification accuracy for the methods used for EV fault diagnosis. The proposed WG-Sparse-ACTNet model reached 99%, followed by IB-DRN (98%) [21], ANN (97.80%) [11], GA-ELM (96.65%) [12], DMGWO-SVM (96.50%) [20], BO-SVDD (94%) [17], and GA-RF (91.12%) [18]. These results indicate proposed technique achieved a better ability to classify faults compared to traditional methods and hybrid methods.

Fig. 17 contains two graphs that provide the precision and recall percentages for selected models. In the precision graph, the proposed model achieved 98% precision, followed by ANN (97%) [11], GA-RF (91%) [18], and IB-DRN (94%) [21]. In the recall graph, the proposed model achieved 98% recall, followed by IB-DRN (97%), ANN (97%), and GA-RF (92%). The outcomes established a proposed model able to identify EV faults reliably with high sensitivity and accuracy.

***Table 3**: Comparison of F1-Score.*

METHODS	F1-SCORE
GA-RF [18]	91%
IB-DRN [21]	94%
ANN [11]	97%
PROPOSED	98%

Table 3 shows the F1-score values for the various methods. The proposed model showed the highest F1 score of 98%, while ANN is 97%, IB-DRN is 94%, and GA-RF is 91%, indicating the strong classification effectiveness in handling complex fault patterns in EV.

Table 4 contains a class-wise assessment of the proposed WG-Sparse ACTNet model. The model achieves accurate classification in the Normal-0 and Battery Fault-1 classes, with precision, recall, and F1-score values of 1.00. The model obtains a precision of 0.97, recall of 0.95, and F1-score of 0.96 for the Motor Fault-2 class, and an F1-score of 0.97 for the Sensor Fault-3 class. The suggested model has an overall classification accuracy of 0.99, with macro-average precision, recall, and F1-score values

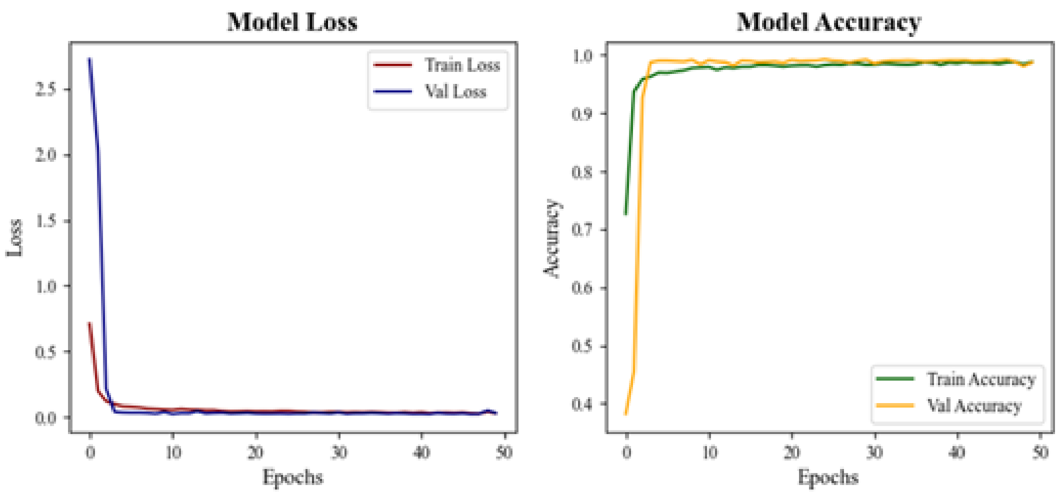

Fig. 12: Model Loss and Accuracy.

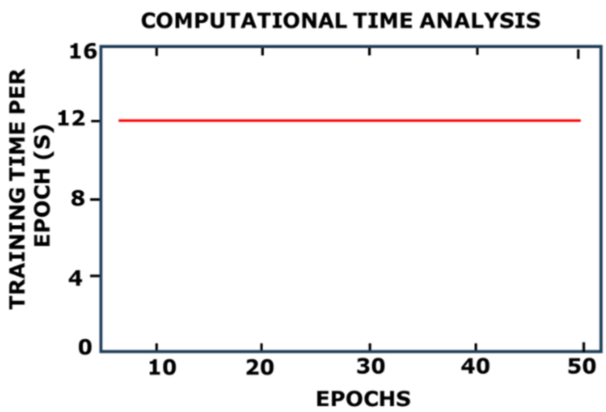

Fig. 13: Computational time analysis.

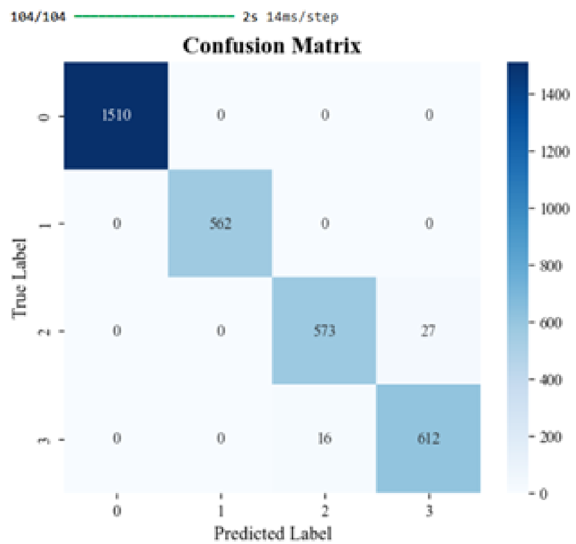

Fig. 14: Confusion Matrix.

of 0.98, indicating that the proposed framework for identifying issues in EVs is highly durable and reliable.

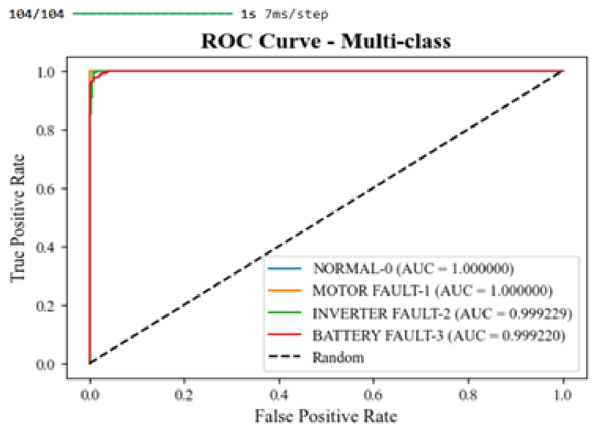

Fig. 15: ROC curve.

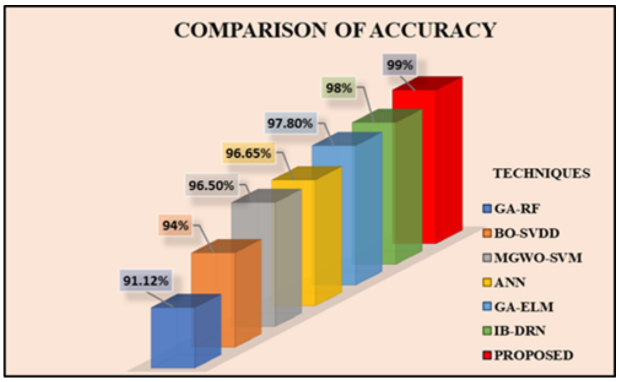

Fig. 16: Comparison of accuracy.

Fig. 18 depicts class-wise F1-score performance of the WG-Sparse ACTNet model. The Normal-0 and Battery Fault-1 classifications have the greatest F1 score (??), signifying perfect categorization. The Motor Fault-2 class has an F1 score of 0.96, and the Sensor Fault-3 class has an F1 score of 0.97. These results demonstrate the proposed model's consistent and superior fault classification

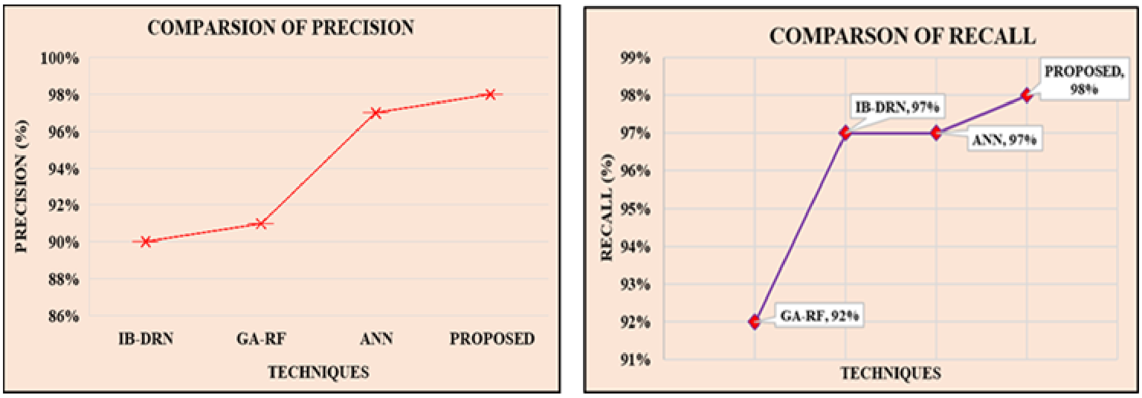

***Fig. 17**: Comparison of precision and recall.*

***Table 4**: Class-wise Performance evaluation.*

	Precision	Recall	F1-score
Normal-0	1.00	1.00	1.00
Battery Fault-1	1.00	1.00	1.00
Motor Fault-2	0.97	0.95	0.96
Sensor Fault-3	0.96	0.97	0.97
Accuracy	0.99		
Macro avg	0.98	0.98	0.98

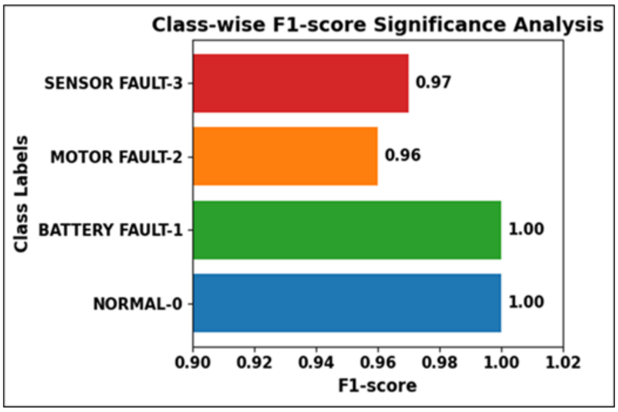

***Fig. 18**: Class-wise F1-score analysis.*

capacity across all categories.

4. CONCLUSION

This study introduces a highly efficient, optimized DL-based architecture for the accurate FDD in EVs through the use of the WG-Sparse-ACTNet model. Systematic data preprocessing helps to maintain the dataset's quality and consistency prior to training. EDA assists in revealing hidden trends and variable relationships, while feature engineering aids in extracting informative characteristics that improve the learning process. With the aid of the proposed model, which includes sparse convolutional and attention-based techniques to focus on salient features when performing classification. WGOA effectively tunes the hyperparameters to maximize model performance. Using the NEV Fault Testing Dataset and implemented on the Python platform, the proposed model achieves 99% accuracy and 98% precision, recall, and F1 score. The proposed model overcomes the limitation of traditional diagnostic approaches by enabling real-time, accurate, and reliable fault classification. Furthermore, the proposed structure decreases false alarms, increases generalization capability, and facilitates predictive maintenance, proving its high potential for the advancement of intelligent EV diagnostic systems.

REFERENCES

[1] M. Z. Khaneghah, M. Alzayed and H. Chaoui, “Fault detection and diagnosis of the electric motor drive and battery system of electric vehicles,” *Machines*, vol. 11, no. 7, pp. 713, Jul. 2023.

[2] C. Wu, R. Sehab, A. Akrad and C. Morel, “Fault diagnosis methods and fault tolerant control strategies for the electric vehicle powertrains,” *Energies*, vol. 15, no. 13, pp. 4840, Jul. 2022.

[3] K. S. Kavin, P. S. Karuvelam, A. Pathak, T. R. Premila, R. Hemalatha and T. Kumar, “Modelling and analysis of hybrid fuzzy tuned PI controller based PMBLDC motor for electric vehicle applications,” *SSRG International Journal of Electrical and Electronics Engineering*, vol. 10, no. 2, pp. 8-18, Feb. 2023.

[4] S. Sandhiya and I. Abinaya, “Experimental analysis on different effects of PV module with respect to panel angle using machine learning algorithms,” *information technology in industry*, vol. 9, no. 3, pp. 367-374, Apr. 2021.

[5] D. Li, Z. Zhang, P. Liu, Z. Wang and L. Zhang, “Battery fault diagnosis for electric vehicles based on voltage abnormality by combining the long short-term memory neural network and the equivalent circuit model,” *IEEE transactions on power electronics*, vol. 36, no. 2, pp. 1303-1315, Jul. 2020.

[6] N. Kumarasabapathy, K. S. Kavin, K. Sakthidhasan, G. W. Martin, S. Gr and T. Nadu, “Optimized Speed and Current Controller Based High Speed Switched Reluctance Motor for EV Applications”,

Futuristic Trends in Electrical Engineering, IIP Series, vol. 3, Book 1, Part2, Chapter 3, 2024.

[7] V. Vaishnavi, and A. Inbamani, "Perturb and Observe Algorithm Based MPPT Controller for a Stand-Alone PV System Using Iot and Machine Learning Algorithms", *International Research Journal of Modernization in Engineering Technology and Science*, 2021.

[8] K. M. Sundaram, A. Hussain, P. Sanjeevikumar, J. B. Holm-Nielsen, V. K. Kaliappan and B. K. Santhoshi, "Deep learning for fault diagnostics in bearings, insulators, PV panels, power lines, and electric vehicle applications—the state-of-the-art approaches," *IEEE Access*, vol. 9, pp. 41246-41260, Mar. 2021.

[9] V. Veerasamy, N. I. Abdul Wahab, A. Vinayagam, M. L. Othman, R. Ramachandran, A. Inbamani and H. Hizam, "A novel discrete wavelet transforms based graphical language classifier for identification of high impedance fault in distribution power system," *International Transactions on Electrical Energy Systems*, vol. 30, no. 6, pp. e12378, Jun. 2020.

[10] C. S. Wang, I. H. Kao and J. W. Perng, "Fault diagnosis and fault frequency determination of permanent magnet synchronous motor based on deep learning," *Sensors*, vol. 21, no. 11, pp. 3608, May 2021.

[11] D. P. Mishra, S. S. Padhy, P. S. Pradhan, S. Gupta, A. Senapati and S. R. Salkuti, "Fault detection and diagnosis of electric vehicles using artificial intelligence," *International Journal of Applied*, vol. 13, no. 3, pp. 653-660, Sep. 2024.

[12] L. Yao, S. Xu, Y. Xiao, J. Hou, X. Gong, Z. Fu and A. Tang, "Fault identification of lithium-ion battery pack for electric vehicle based on GA optimized ELM neural network," *IEEE Access*, vol. 10, pp. 15007-15022, Jan. 2022.

[13] M. U. I. Khan, M. I. H. Pathan, M. M. Rahman, M. M. Islam, M. A. R. Chowdhury, M. S. Anower, M. M. Rana, M. S. Alam, M. Hasan, M. S. I. Sobuj and M. B. Islam, "Securing electric vehicle performance: Machine learning-driven fault detection and classification," *IEEE Access*, vol. 12, pp. 71566-71584, May 2024.

[14] M. Aishwarya and R. M. Brisilla, "Design and fault diagnosis of induction motor using ML-based algorithms for EV application," *IEEE Access*, vol. 11, pp. 34186-34197, Mar. 2023.

[15] H. Kaplan, K. Tehrani and M. Jamshidi, "A fault diagnosis design based on deep learning approach for electric vehicle applications," *Energies*, vol. 14, no. 20, pp. 6599, Oct. 2021.

[16] K. S. K. Chu, K. W. Chew, Y. C. Chang and S. Morris, "An Open-Circuit Fault Diagnosis System Based on Neural Networks in the Inverter of Three-Phase Permanent Magnet Synchronous Motor (PMSM)," *World Electric Vehicle Journal*, vol. 15, no. 2, pp. 71, Feb. 2024.

[17] J. Yang, F. Cheng, M. Duodu, M. Li and C. Han, "High-precision Fault Detection for electric vehicle battery system based on bayesian optimization SVDD," *Energies*, vol. 15, no. 22, pp. 8331, Nov. 2022.

[18] R. N. Toma, A. E. Prosvirin and J. M. Kim, "Bearing fault diagnosis of induction motors using a genetic algorithm and machine learning classifiers," *Sensors*, vol. 20, no. 7, pp. 1884, Mar. 2020.

[19] W. Zheng and T. Wang, "Electric vehicle motor fault diagnosis using improved wavelet packet decomposition and particle swarm optimization algorithm," *Archives of Electrical Engineering*, pp. 481-498, 2024.

[20] L. L. Li, J. Q. Liu, W. B. Zhao and L. Dong, "Fault diagnosis of high-speed brushless permanent-magnet DC motor based on support vector machine optimized by modified grey wolf optimization algorithm," *Symmetry*, vol. 13, no. 2, pp. 163, Jan. 2021.

[21] V. S. R. Kosuru and A. Kavasseri Venkitaraman, "A smart battery management system for electric vehicles using deep learning-based sensor fault detection," *World Electric Vehicle Journal*, vol. 14, no. 4, pp. 101, Apr. 2023.

V. Suresh is working as an Assistant Professor in School of Engineering, Department of Electrical and Electronics Engineering at Godavari Global University, Rajahmundry, Andhra Pradesh, India. I have secured Ph.D. in Electrical Engineering at JNTUA University, Anantapur, Andhra Pradesh, India. I have more than 14 years of teaching experience and good publication record includes 6-SCIE indexed journals, 45-Scopus indexed journals, 12-International/National Conferences and 57 - patents. My research area includes Hybrid Electric Vehicles, Renewable Energy Systems, Micro grids and Power Electronics.

Ch. Leela Kumari is working as an Assistant Professor in the Department of Electrical and Electronics Engineering at Godavari Institute of Engineering and Technology (Autonomous), Rajahmundry, Andhra Pradesh, India. She completed Ph.D. in Electrical Engineering at Lovely Professional University, Punjab, India. She is in Teaching Profession for more than 12 years. She has presented 17 research papers in National, International Journals & Conference and Published 7 Patents. Her main area of interest includes Power Systems, Electric Vehicles, and Renewable Energy Systems, and she is working on MSME project currently.

Marise Satheesh is studying in department of Electrical and Electronics Engineering in Godavari Institute of Engineering and Technology (A), Rajahmundry from Jawaharlal Nehru Technological University, Kakinada.

Vuyyuru Sri Kavya is studying in department of Electrical and Electronics Engineering in Godavari Institute of Engineering and Technology (A), Rajahmundry from Jawaharlal Nehru Technological University, Kakinada.

Nukarapu V V L N Pavani is studying in department of Electrical and Electronics Engineering in Godavari Institute of Engineering and Technology (A), Rajahmundry from Jawaharlal Nehru Technological University, Kakinada.